

## PHYSICO-CHEMICAL CHARACTERISTICS OF THE VITRIFIED SIMULATED HLW AT EDC MCC

Aloy A. S., Trofimenko A. V., Koltsova T. I., Nikandrova M. V.

JSC Khlopin Radium Institute, Saint-Petersburg, Russia

Article received on October 25, 2018

---

*The paper overviews the results of experiments assessing some quality indicators of borosilicate glass matrix with its composition designed to condition liquid high-level waste resulting from WWER-1000 SNF reprocessing applying basic PDC MCC (Zhelesnogorsk) technology. These investigations were prompted by the need of adding specific technical data to relevant legal framework on RW management concerning borosilicate glass matrix being considered as an alternative to the aluminophosphate one.*

**Key words:** borosilicate glass, high level waste, quality indicators, mechanical properties, crystallization, leachability.

### Introduction

Ensuring the environmental safety is viewed as the main task in the management of continuously generated radioactive waste (RW). This goal is being attained by ensuring the compliance of RW physical and chemical characteristics with relevant requirements of the Unified State System for RW Management (USS RW) being established in the Russian Federation [1].

General requirements are being set under the USS RW development to ensure safe and cost-efficient mechanisms for its operation. For this purpose, relevant regulations are being developed and reviewed with due account of the development and implementation of new technologies and SNF/RW processing products.

In keeping with Article 26, para 2 of the Federal Law № 190 On Radioactive Waste Management and Introducing Some Amendments to Particular Legal Acts of the Russian Federation (2011), all newly generated liquid RW shall be considered as retrievable. Such waste should be disposed of in purpose designed disposal facilities following waste

conditioning resulting in a solid form complying with relevant acceptance criteria for disposal.

Acceptance criteria set for most hazardous immobilized HLW forms are established based on the acceptable values describing the chemical stability and specific heat generation, SRW heat removal conditions, as well as relevant characteristics of the storage facility and the bedrocks of the planned final disposal facility [2].

Acceptance evaluations are based on the key quality indicators of the immobilized liquid RW. Relevant indicators set for glasslike matrixes are discussed in the new draft of federal norms and rules in the field of atomic energy use, namely, Collection, Processing, Storage and Conditioning of Liquid Radioactive Waste: Safety Requirements approved by order of the Federal Service for Environmental, Technological and Atomic Supervision (NP-019-2015).

The first edition of NP-019-2000 featured the acceptable values for a number of quality indicators exclusively for aluminophosphate glasses.

Advances associated with new liquid HLW vitrification technologies have prompted the need for the development of similar requirements on borosilicate matrixes being considered as a preferable option abroad with a big amount of scientific and technical data being accumulated to date [3, 4].

The experimental study suggested as its goal a series of tests to investigate physical and chemical properties of simulated borosilicate glass samples designed to condition liquid HLW resulting from the full cycle application of the basic WWER-1000 SNF reprocessing technology at the PDC MCC. The results obtained, as well as data from international literature sources may be used to demonstrate a specific set of main borosilicate glass quality indicators during the development of the new regulations.

Synthesis of borosilicate glasses containing simulated PDC MCC HLW

To evaluate main quality indicators for borosilicate glasslike compound, glasses containing 15 and 20% of model HLW oxides by mass (BSS-15 and BSS-20) were manufactured (table 1). The calculations show that such high inclusion of waste results in approximately 100–110 dm<sup>3</sup> of high-level glass from 1 ton of reprocessed SNF. Based on the initial data on the basic SNF reprocessing technology, simulated HLW also contained stainless steel corrosion products (Fe, Cr, Ni) and sodium from washing and extractant regeneration.

**Table 1. Calculated composition of simulated glasses BSS-15 and BSS-20, % by mass**

Oxides	BSS-15	BSS-20
SiO <sub>2</sub>	48.45	45.60
B <sub>2</sub> O <sub>3</sub>	15.30	14.40
Al <sub>2</sub> O <sub>3</sub>	2.55	2.40
Na <sup>2</sup> O	13.44	13.35
CaO	2.55	2.40
Fe <sub>2</sub> O <sub>3</sub>	0.19	0.25
NiO	0.09	0.12
Cr <sub>2</sub> O <sub>3</sub>	0.54	0.72
Li <sub>2</sub> O	2.98	2.80
MnO <sub>2</sub>	2.55	2.40
FP oxides*	11.38	15.14
SiO <sub>2</sub> + B <sub>2</sub> O <sub>3</sub> + Al <sub>2</sub> O <sub>3</sub>	66.30	62.40

\*FP – fission products

Glass melting was performed in a muffle furnace at a temperature of (1150 ± 20) °C with 2 hours long melt exposure.

The following methods were applied to evaluate the homogeneity and compliance of BSS composition with the calculated values:

- X-ray phase analysis (XRF) (diffractometer DRON-UM1 applying CuKα-radiation);
- scanning electron microscopy (SEM);
- X-ray microanalysis (RSMA) (CAMSCAN-4DV electron microscope equipped with LINKAN-10000 system). Microanalysis data processing was performed using ZAF4/FLS software;
- microhardness test.

### Homogeneity

Preliminary evaluation of the synthesized glasses was carried out by the XFA method according to GOST R 50926-96 provisions [5]. XFA data allowed to state that all BSS could be considered as X-ray amorphous and did not contain dispersed phases. A more detailed homogeneity study was carried out by repeated measuring of the main components content in the glasses by the RSMA method: Na, Al, Si, Ca, Mn, Sr, Cs, La, Zr. The homogeneity characteristic was calculated based on the following equation:

$$K = \frac{S}{\bar{x}} \cdot 100 \%, \quad (1)$$

where  $K$  is variation coefficient reflecting the degree to which the content of the considered glass component deviates from its average content in glass, %;  $S$  is the mean-square deviation allowing to estimate the absolute dispersion of the values;  $\bar{x}$  – average content of the considered component in glass.

Table 2 summarizes the data obtained.

**Table 2. Homogeneity characteristics of the studied glasses**

Oxide	Variation coefficient, %	
	BSS-15	BSS-20
Na <sub>2</sub> O	2.65	2.32
Al <sub>2</sub> O <sub>3</sub>	7.44	9.13
SiO <sub>2</sub>	1.72	2.42
CaO	6.25	5.10
MnO <sub>2</sub>	7.94	8.30
SrO	10.00	9.92
Cs <sub>2</sub> O	9.96	9.96
La <sub>2</sub> O <sub>3</sub>	8.26	8.04
ZrO <sub>2</sub>	9.42	8.61

Homogeneity of glass by the macro component content does not exceed 10% including main heat generating nuclides Cs and Sr, thus, providing a homogeneous distribution of waste components in the glass matrix.

Additional evaluations of BSS-15 and BSS-20 quality were performed by measuring the microhardness of polished sections using a standard method: diagonal of residual prints on the glass surface was measured after indenter insertion, namely, a Vickers pyramid with a  $136^\circ$  vertex angle, performed at microhardness meter PMT-3 (load – 0.98 N, loading time – 10 s) [6]. Microhardness was calculated based on the following equation:

$$H = \frac{1854P}{d^2}, \quad (2)$$

where  $H$  is hardness, GPa,  $P$  – load on indenter, N,  $d$  – print diagonal, micron.

The following microhardness values were obtained based on the experiments performed (45 measurements):  $(7.1 \pm 0.3)$  GPa for BSS-15 glass and  $(7.6 \pm 0.5)$  GPa for BSS-20 glass. Minor scattering of BSS microhardness parameters demonstrates the homogeneity of the studied glasses both in terms of their composition and structure.

### Mechanical properties

Glass is believed to be quite a fragile material and its stability under the impact of mechanical factors is viewed as an important criterion in the evaluation of the physical stability of the immobilized waste form. Inside radioactive glass block, internal stresses are caused by the presence of a temperature gradient between its center and its surface. This gradient decreases with time, but persists for hundreds of years until the decay of the main heat generating radionuclides. Internal thermal stresses cause the formation of cracks and ultimately can lead to self-induced destruction of the glass block. Cracking increases the surface area of the glass,

thereby increasing the possibility of increased leaching and release of radionuclides into the environment. Mechanical forces (pressure, bending, torsion, and etc.) acting on the glass container (for example, inside a geological formation) can not only cause its breaking, but also break its contents into small particles.

In this regard, the mechanical properties of vitrified RW certainly require quantitative regulation, and relevant values should meet the acceptance criteria set for RW storage and disposal.

Pre-sampling efforts were performed in keeping with the requirements of instrumental testing methods, thus, BSS-15 and BSS-20 were melted in a platinum dish at a temperature of  $1,150^\circ\text{C}$  and poured into preheated stainless-steel forms. These sample containing forms were put into a furnace, where they were held at temperature of  $420^\circ\text{C}$  for 4 hours for annealing purposes followed by form and furnace cooling to ambient temperature.

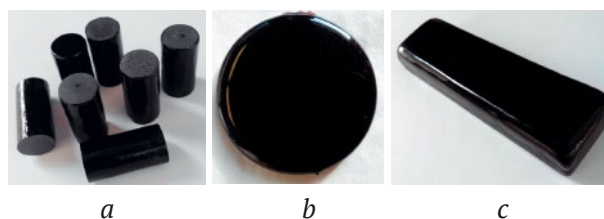


Figure 1. Glass samples for various testing methods: a – compressive strength and Young's modulus; b – bending strength and heat resistance; c – coefficient of linear thermal expansion

Figure 1 shows the glass samples manufactured for the testing purposes listed in table 3.

Figure 2 shows the equipment applied to measure a number of borosilicate glass quality indicators given in Table 3.

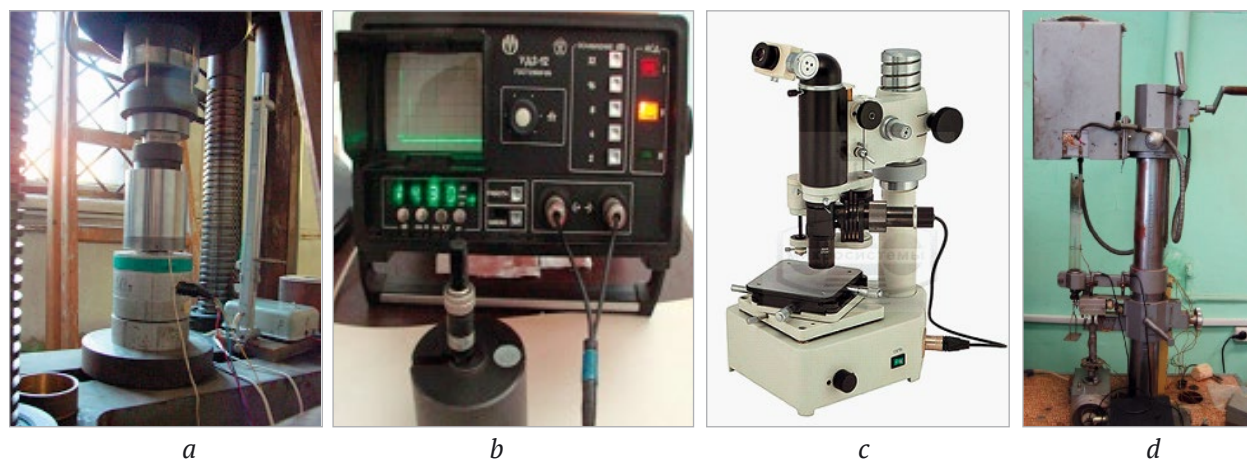


Figure 2. Equipment applied to measure the main borosilicate glass quality indicators: a – GMS-50 press, b – UD2-12 flaw detector, c – PMT-3 microhardness meter, d – Klyuev-Chernousov system quartz dilatometer-viscometer

Table 3. Identified characteristics, materials and testing methods

Identified characteristic	Testing method	Applied equipment	Sample dimensions
Microhardness	GOST 9450-76 [6]	microhardness tester PMT-3 (figure 2c)	8 mm high plates with a diameter of 50 mm
Density	GOST 2409-95 (ISO 5017-88) [7]	analytical balance OHAUSE 12140	plane-parallel cylindrical 25 mm high samples with a diameter of 10 mm
Young's modulus	GOST R 53568-2009 [8]	flaw detector UD2-12 (figure 2b)	cylindrical 25 mm high samples with a diameter of 10 mm
Compression resistance	GOST R 50926-96 [5]	press GMS-50 (figure 2a)	cylindrical 25 mm high samples with a diameter of 10 mm
Flexing strength	GOST 32281.1-2013 (EN 1288-1:2000) [9]	Press GMS-50, load gauge DS-1	4 mm high plates with a diameter of 70 mm
Thermal resistance	GOST 25535-2013 In keeping with para. 8.4, B [10]	SNOL 24-200	Round 4 mm thick plates with a diameter of 70 mm
Thermal linear expansion coefficient	dilatometric analysis	Klyuev-Chernousov systems quartz dilatometer- viscometer (figure 2d)	beams (12 × 2 × 1 cm)

### Density

Glass density ( $\rho$ ) was determined based on hydrostatic weighing method [7]. The density was calculated using the following equation:

$$\rho = \frac{m_0}{(m_1 - m_2)}, \quad (3)$$

where  $m_0$  is the sample mass,  $m_1$  – mass of the sample with a suspender,  $m_2$  – mass of the sample in water.

Based on the tests conducted, it was found that the density of borosilicate glass BSS-15 and BSS-20 accounts for 2.68 g/cm<sup>3</sup> and 2.76 g/cm<sup>3</sup> respectively.

### Elastic behavior (Young's modulus)

Elastic behavior of the studied glasses was evaluated using acoustic (ultrasonic) method with UD 2-12 flaw detector [8]. Data on the speed of longitudinal ( $C_l$ , km/sec) and transverse ( $C_t$ , m/sec) acoustic wave propagation in the studied samples was used to calculate the following values associated with the elastic behavior (Table 4):

Modulus of longitudinal elasticity:

$$C_{ll} = \rho \cdot C_l^2. \quad (4)$$

Shear modulus

$$G = \rho \cdot C_t^2. \quad (5)$$

Poisson's ratio ( $\mu$ )

$$\mu = \frac{(C_l/C_t)^2 - 2}{2[(C_l/C_t)^2 - 1]}. \quad (6)$$

Young's modulus

$$E = C_{ll} \cdot \frac{(1 + \mu) \cdot (1 - 2\mu)}{(1 - \mu)}. \quad (7)$$

Volumetric modulus of elasticity

$$K = C_{ll} \cdot \frac{1 + \mu}{3(1 - \mu)}. \quad (8)$$

Table 4. Elastic characteristics of the studied glasses

Parameter	BSS-15	BSS-20
Modulus of longitudinal elasticity, GPa	98 ± 3	100 ± 3
Shear modulus, GPa	32 ± 3	33 ± 3
Poisson's ratio	0.26 ± 0.01	0.25 ± 0.01
Young's modulus, GPa	80 ± 3	83 ± 3
Volumetric modulus of elasticity, GPa	56 ± 3	56 ± 3

For BSS-15 and BSS-20, Young's modulus values are almost two times higher than those set forth by relevant provisions of NP-019-20003 for aluminophosphate glasses.

### Strength characteristics

Compressive strength of the studied glasses was determined using GMS-50 press [5]. The pressing force was measured by applying two methods: a) roughly, according to the scale of the press, b) accurately – using a strain gauge with an accuracy of ± 1%. Loading time accounted for 20 seconds. The calculation of compressive strength was carried out using the following equation:

$$\sigma_f = \frac{P_f}{S}, \quad (9)$$

where  $\sigma_f$  is compressive strength, GPa;  $P_f$  – breaking strength, kN;  $S$  – sample's cross-section area, mm<sup>2</sup>.

The following compressive strength values were obtained for the studied glass samples based on the tests conducted: (0.8 ± 0.2) GPa for BSS-15 glass and (1.4 ± 0.5) GPa for BSS-20 glass. The force associated with flexing strength of the studied glass samples was measured using DS-1 model dynamometer [9]. The measurement accuracy accounted for ± 1% with a loading time of 20 seconds.

Flexing strength was calculated using the following equation:

$$\sigma = \frac{3P_f}{2\pi h^2} \cdot \left[ (1+\mu) \ln \frac{a}{r_0} + (1-\mu) \cdot \frac{a^2 - r_0^2}{2b^2} \right], \quad (10)$$

where  $P_f$  stands for the breaking strength, N,  $h$  — thickness of the glass plate, mm;  $a$  — radius of the lower support, mm;  $r_0$  — radius of the loading ring, mm;  $b$  — radius of the glass plate, mm.

The tests have demonstrated that the flexing strength of the studied glass samples BSS-15 and BSS-20 are equal accounting for  $(0.16 \pm 0.07)$  GPa.

### Thermal and physical properties

Thermal and physical characteristics of glasses are believed to be important in terms of the safety assessment associated with can transportation and subsequent long-term storage under elevated temperature conditions providing that no uncontrolled glass transformations can occur causing speedy increase of glass component leachability rate.

#### Thermal resistance

Thermal resistance is viewed as the ability of glass and glass products to withstand sudden temperature fluctuation without degradation.

This parameter is not included to the list of quality indicators set for RW containing glass. However, in certain cases, especially during transportation, its value can also be taken into account.

Relevant testing method suggested that glass samples were heated up to a certain temperature in SNOL 24-200 furnace. These were held under this temperature for 20 minutes and then instantly discharged into cold water with a temperature of  $(19 \pm 1)^\circ\text{C}$  and cooled there for 40 seconds. After that, the samples were removed from the water and dried. Visual inspection was performed. If no signs of such degradation were observed, the samples were put again to the furnace where the temperature was increased by  $10^\circ\text{C}$ . These operations were recurrently done till the glass samples were destroyed [10]. The temperature difference ( $T = T_{hot} - T_{cold}$ ) associated with sample destruction was taken as the value of the thermal resistance parameter. The tests have demonstrated that heat resistance values for BSS-15 and BSS-20 samples are equal accounting for  $(151 \pm 1)^\circ\text{C}$ , which are viewed as favorable indicators in terms of glass technology.

#### Linear thermal expansion coefficient

Linear thermal expansion coefficient (LTEC) was determined based on dilatometric method using a quartz dilatometer-viscometer of V. P. Klyuev-M. A. Chernousov system.

LTEC  $\alpha_g$  ( $^\circ\text{C}^{-1}$ ) was calculated using the following equation:

$$\alpha_g = \frac{\Delta L}{L_0 \Delta T}, \quad (11)$$

where  $\Delta L$  accounts for the change in the length of the studied glass sample ( $\mu\text{m}$ ) when heated in a temperature range of  $\Delta T$  ( $^\circ\text{C}$ ),  $L_0$  accounts for the initial length of the sample ( $\mu\text{m}$ ). Temperature range  $\Delta T$  ( $^\circ\text{C}$ ) was chosen based on a dilatometric curve, namely, the area lying below the glass transition temperature  $T_g$ . In this temperature range (300–450  $^\circ\text{C}$ ) the viscosity of glass becomes equal to  $10^{13}$  poises. Measurements were carried out under heating — cooling cycles with a rate of temperature change accounting for  $3^\circ\text{C}/\text{min}$ .

The calculated LTEC values for BSS-15 and BSS-20 accounted for  $(10.5 \pm 0.3) \cdot 10^{-6}^\circ\text{C}^{-1}$  and  $(11.8 \pm 0.1) \cdot 10^{-6}^\circ\text{C}^{-1}$  respectively.

#### Thermal stability

Theoretically, when heated a more thermodynamically stable state of glass can be achieved due to the formation of crystalline phases. However, such devitrification process proceeds extremely slowly or cannot even be implemented at all if the glass is held under the temperatures being below the values required for such a transformation [3]. Benchmark applied in France for long-term storage of eurocans with vitrified HLW has shown that the temperature in the central zone of a BSS glass block should be  $100^\circ\text{C}$  below the devitrification temperature due to intensive cooling of the can's walls [11].

In our case study, thermal resistance to devitrification was investigated on BSS-20 sample.

Differential thermal analysis (DTA) of the BSS-20 sample was carried out using derivatograph Evo-1750 (Setaram, France) operated using argon media at a heating and cooling rate of  $10^\circ\text{C}/\text{min}$ . When heated, the maximum crystallization peak for BSS-20 glass corresponded to a temperature of  $618^\circ\text{C}$ , when cooled — to a temperature of  $632^\circ\text{C}$  (Figure 3)

An average value of  $(625 \pm 10)^\circ\text{C}$  was calculated taking into account the hysteresis loop.

It's assumed that a decrease in this value by  $100^\circ\text{C}$ , according to [11], suggested that for a rather long time period crystallization process at a temperature of  $(525 \pm 10)^\circ\text{C}$  will not proceed at any appreciable rate.

Long-term storage of cans containing highly active BSS (Figure 4) should be arranged in a way suggesting that the requirement on non-exceedance of the characteristic temperature in the can center is observed. Such conditions should be ensured by intense air cooling of the walls of cans held at storage racks.

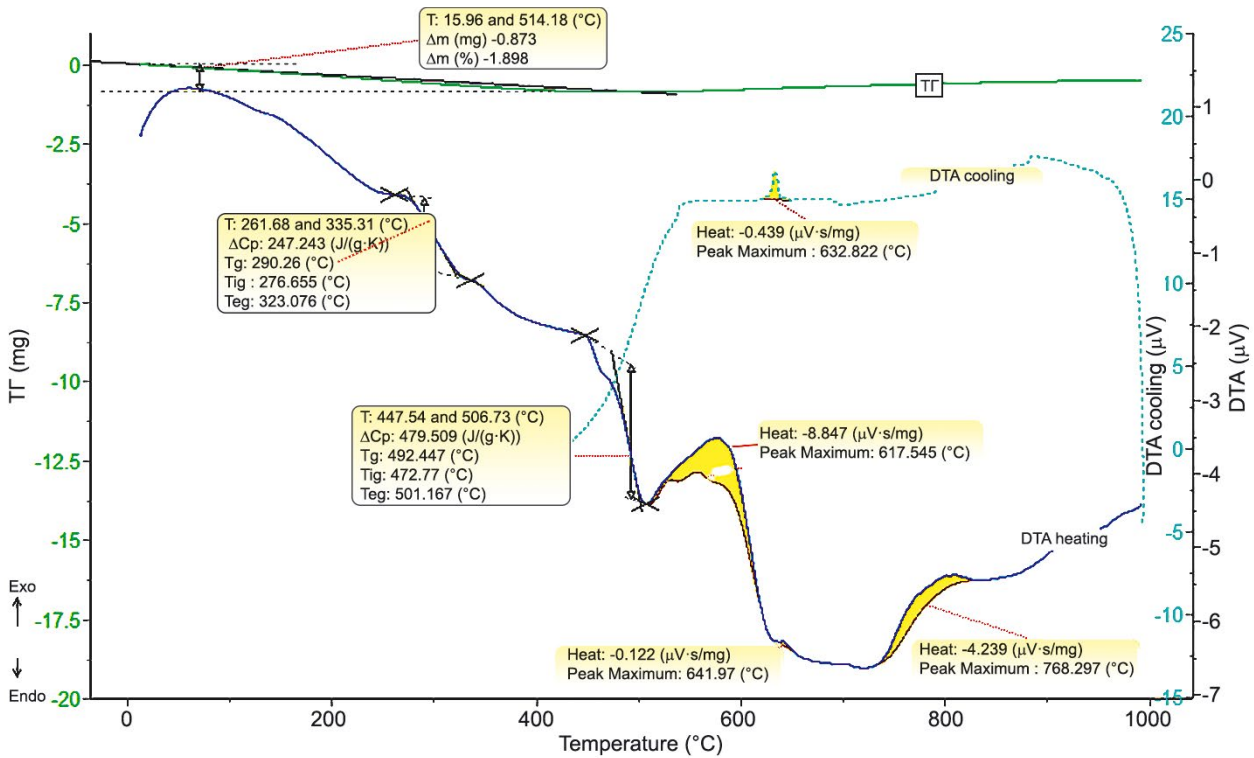


Figure 3. Thermogram for BSS-20 borosilicate glass sample

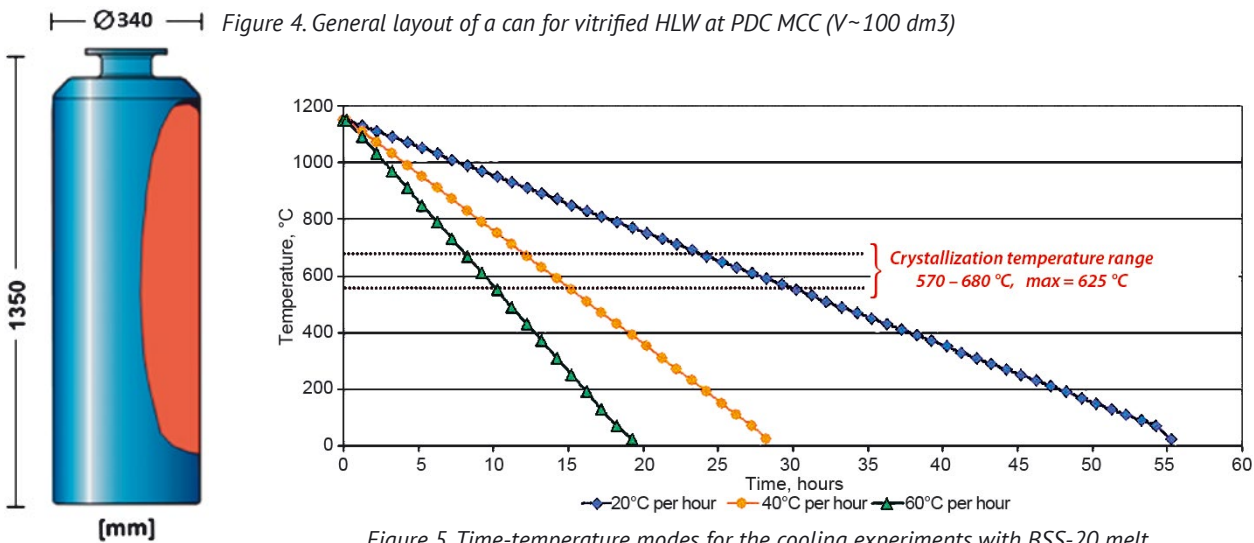


Figure 5. Time-temperature modes for the cooling experiments with BSS-20 melt

Relationships between the crystallization and the cooling rate for BSS-20 melt suggested as can’s filling medium were studied. The experimental technique suggested that a glass sample was placed into an aluminum crucible and held in a SNOL muffle furnace at a temperature of 1,150°C for 15 minutes. Then the heating was stopped, and the melt containing crucible was cooled down to ambient air temperature for a predetermined period of time. The cooling rate of the glass melt accounted for 20, 40 and 60°C/h. Time-temperature dependencies are shown in Figure 5.

The cooled crucible was cut along its axis and its physical and chemical properties were further studied using EPMA and SEM methods.

Figure 5 shows that the time corresponding to the temperature range with the melt being undergoing the crystallization process is inversely proportional to the cooling rate (Table 5).

Table 5. Time period corresponding to the temperature range of 570–680 °C depending on the glass sample cooling rate

Cooling rate, °C/hours	Cooling time, hours
20	6
40	3
60	2

Study of samples morphology and composition has shown that crystalline phase was only present in the sample cooled at a rate of 20 °C/h (Figure 6). The content of crystalline inclusions did not exceed 0.2 vol%, with an average particle size of 1.6 μm.

EMPA indicated the following crystalline phase content (mass %): SiO<sub>2</sub> – 68.0; Na<sub>2</sub>O – 20.5; CaO – 5.7; La<sub>2</sub>O<sub>3</sub> – 5.8.

Thus, even at a minimum cooling rate of the glass melt (20 °C/h), this temperature range will be overcome fast enough so that no significant transformations of the glass-like matrix could take place and, thus, no significant reduction in the vitrified RW chemical stability is expected.

### Chemical stability

Chemical stability of the synthesized glasses was evaluated in keeping with GOST 52126–2003 provisions [12] using cylinder-shaped samples with a volume of ≈ 1 cm<sup>3</sup> and at temperatures ranging from (20 ± 3) to (90 ± 3) °C. Tests were carried out at increased temperatures using SNOL 24/200 compartment drier installed in purposely designed autoclaves.

Elemental composition of the leached solutions was evaluated using Inductively Coupled Plasma Atomic Emission Spectrometer (ICP-AES) Varian 725-ES. Mathematical processing of the experimental data on leaching enabled to obtain the values of standardized leaching  $N_L(i)$  (g/m<sup>2</sup>) (mass loss) and leaching rate  $R_L(i)$  (g/cm<sup>2</sup>·day) for the vitrified HLW components:

$$N_L(i) = \frac{m_i}{f_i \cdot S}, \quad (12)$$

$$R_L(i) = \frac{dN_L(i)}{dt} = \frac{1}{f_i \cdot S} \cdot \frac{dm_i}{dt}, \quad (13)$$

where  $m_i$  – total amount of  $i$ -component in the leached solution (g),  $S$  – surface area interacting with contact solution (m<sup>2</sup>),  $f_i$  – mass fraction of  $i$ -component in glass.

Equilibrium leaching rate values for the components contained in the studied glasses are given in Table 6.

**Table 6. Chemical stability of the studied glasses**

Glass	BSS-15		BSS-20	
Leaching temperature, °C	20 ± 3	90 ± 3	20 ± 3	90 ± 3
RL(Cs), g/(cm <sup>2</sup> ·day)	2.15·10 <sup>-7</sup>	8.60·10 <sup>-6</sup>	2.18·10 <sup>-7</sup>	8.72·10 <sup>-6</sup>
RL(Sr), g/(cm <sup>2</sup> ·day)	5.25·10 <sup>-8</sup>	2.10·10 <sup>-6</sup>	4.98·10 <sup>-8</sup>	1.99·10 <sup>-6</sup>

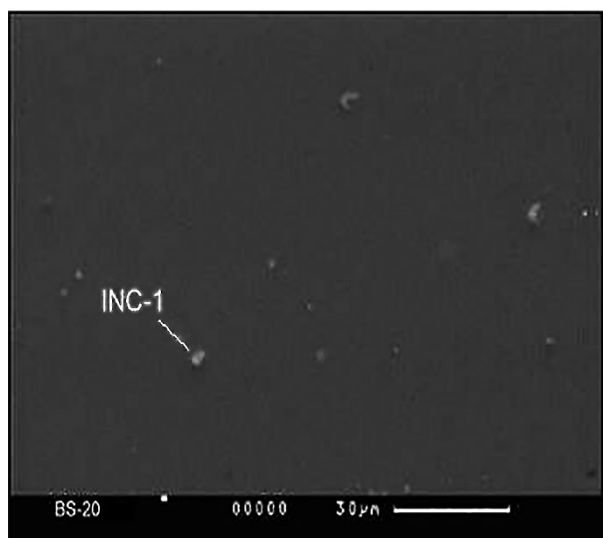


*Figure 6. SEM-photomicrography of BSS-20 sample at a cooling rate of 20 °C per hour*

More details on the processes associated with BSS interaction with different water solutions including formation of surface layers and mathematical modelling of leaching processes can be found in [13–15].

### Conclusion

The paper shows that the quality indicators for BSS-15 and BSS-20 glasses determined based on experimental studies performed using purpose-manufactured samples exceed those specified for phosphate glass-like compounds. For example, for borosilicate glasses, cesium and strontium leaching rates under ambient air temperature are by an order of magnitude less, whereas mechanical compressive and bending strength, as well as elasticity are by an order of magnitude higher. Thermal stability of borosilicate glasses is almost 100 °C higher than the one of aluminophosphate glasses, which is viewed as an important advantage in terms of RW long-term storage.

The results obtained can be used as a basis for amending and supplementing the target quality indicators being discussed under the development of the final version of NP-019-2015 regulation, namely those relevant for borosilicate glasses applied in liquid HLW conditioning practice.

### Acknowledgements

The study was performed under the sponsorship of the State Atomic Energy Corporation Rosatom under the contract (N<sup>o</sup> 25-15-1146/7149/1422) with FSUE MCC.

### References

1. Kriukov O. V. Kratkii kommentarii k utverzhdeniiu "Strategii sozdaniia punkta glubinnogo zakhoroneniia radioaktivnykh otkhodov". *Radioactive Waste*, 2018, no 2 (3), pp. 16–17.
2. NP-093-14. Kriterii priemlemosti radioaktivnykh otkhodov dlia zakhoroneniia. — M.: Rostekhnadzor, 2015. 24 p. HII-093-14.
3. Ozhovan M. I., Pouektov P. P. Stekla dlia immobilizatsii iadernykh otkhodov. *Priroda*, 2010, no. 3, p. 3–11.
4. Gin S., Jollivet P., Tribet M., Peugeot S., Schuller S. Radionuclides containment in nuclear glasses: an overview. *Journal Radiochimica Acta*, 2017, v. 105, p. 927–959.
5. GOST R 50926-96. Otkhody vysokoaktivnye otverzhdannye. Obshchie tekhnicheskie trebovaniia. M.: Gosstandart Rossii, 1996. 3 s..
6. GOST 9450-76. Izmerenie mikrotverdosti vdavlivaniem almaznykh nakonechnikov. — Moscow, Izdatelstvo standartov, 1993. 15 s.
7. GOST 2409-95. Ogneupory. Metod opredeleniia kazhushcheisia plotnosti, otkrytoi i obshchei poristosti, vodopogloshcheniia. Minsk. IPK Izd-vo standartov, oktiabr 2002. 10 s.
8. GOST R 53568-2009. Kontrol nerazrushaiushchii. Opredelenie konstant uprugosti tretego poriadka akusticheskim metodom. Obshchie trebovaniia. — M.: Izdatelstvo standartov, 2010. 10 s.
9. GOST 32281 1-2013 (EN 1288-1:2000). Steklo i izdeliia iz nego. Opredelenie prochnosti na izgib. M.: Standartinform, 2014. 19 s.
10. GOST 25535-2013. Steklo i izdeliia iz nego. Metody opredeleniia termostoikosti. M.: Standartinform, 2014. 8 s.
11. Nuclear Waste Conditioning: monograph / editorial director Philippe Pradel, – Paris: Nuclear Energy Division, 2009. – 145 p. – ISBN 978-2-281-11380-8
12. GOST R 52126-2003. Otkhody radioaktivnye. Opredelenie khimicheskoi ustoichivosti otverzhdenykh vysokoaktivnykh otkhodov metodom dlitel'nogo vyshchelachivaniia. M.: IPK Izd-vo standartov, 2003. 10 s.
13. Aloy A. S., Trofimenko A. V., Kol'tsov a T. I., Nikandrova M. V. Formation of surface layers in leaching of borosilicate glasses incorporating different amounts of simulated HLW. *Radiochemistry*, 2012, vol. 54, iss. 3, pp. 291-297..
14. Aloy A. S., Nikandrova M. V. Leaching of borosilicate glasses containing simulated high-level waste in solutions of hydrogen peroxide as a substance simulating radiolysis products. *Radiochemistry*, 2014, vol. 56, iss. 6, pp. 633-549.
15. Aloy A. S., Nikandrova M. V. Leaching of borosilicate glasses containing simulated high-level waste from the experimental and demonstration center of the mining and chemical combine in mineralized water of a granitoid formation. *Radiochemistry*, 2015, vol. 57, iss. 5, pp. 546-551..

---

### Information about the authors

*Aloy Albert Semenovich*, Doctor of Sciences, chief researcher, JSC Khlopin Radium Institute, (28, 2-nd Murinskiy Avenue, Saint-Petersburg, 194021, Russia), e-mail: aloy@khlopin.ru.

*Trofimenko Alexander Vasilyevich*, Candidate of Chemical Sciences, leading researcher, JSC Khlopin Radium Institute, (28, 2-nd Murinskiy Avenue, Saint-Petersburg, 194021, Russia), e-mail: aloy@khlopin.ru.

*Koltsova Tatyana Ivanovna*, leading engineer, JSC Khlopin Radium Institute, (28, 2-nd Murinskiy Avenue, Saint-Petersburg, 194021), e-mail: koltsova@khlopin.ru.

*Nikandrova Maria Vladimirovna*, Candidate of Chemical Sciences, head of laboratory, JSC Khlopin Radium Institute, (28, 2-nd Murinskiy Avenue, Saint-Petersburg, 194021, Russia), e-mail: nikandrova@khlopin.ru.

### Bibliographic description

Aloy A. S., Trofimenko A. V., Koltsova T. I., Nikandrova M. V. Physico-chemical characteristics of the vitrified simulated HLW at EDC MCC. *Radioactive Waste*, 2018, no. 4 (5), pp. 67–75. (In Russian)